

LARGE VELOCITY GRADIENTS IN THE TIDAL TAILS OF THE INTERACTING GALAXY AM 1353–272 (“THE DENTIST’S CHAIR”)¹

PETER M. WEILBACHER,² UTA FRITZE-V. ALVENSLEBEN,² PIERRE-ALAIN DUC,³ AND KLAUS J. FRICKE²

Received 2002 August 19; accepted 2002 October 1; published 2001 October 9

ABSTRACT

We present Very Large Telescope observations of the interacting system AM 1353–272. Using the FORS2 instrument, we studied the kinematics of the ionized gas along its prominent tidal tails and discovered strikingly large velocity gradients associated with seven luminous tidal knots. These kinematical structures cannot be caused by streaming motion and most likely do not result from projection effects. More probably, instabilities in the tidal tails have led to the formation of kinematically decoupled objects that could be the progenitors of self-gravitating tidal dwarf galaxies.

Subject headings: galaxies: formation — galaxies: individual (AM 1353–272) — galaxies: interactions — galaxies: kinematics and dynamics

On-line material: color figures

1. INTRODUCTION

Interactions among disk galaxies are observed to produce tidal tails of sometimes impressive lengths containing stars and H I in varying proportions. While tidal tails of interacting galaxies have been analyzed in dynamical simulations of interactions to assess their use to probe the form of the dark matter potential (e.g., Springel & White 1999), the detailed kinematics of structures within the tidal tails have not received much attention. Both in deep spectroscopic observations (Duc et al. 2000) and high-resolution dynamical simulations (Barnes & Hernquist 1992), condensations are observed to form in tidal tails, the nature and fate of which are not yet fully understood.

At a distance of 159 Mpc (computed with $H_0 = 75 \text{ km s}^{-1} \text{ Mpc}^{-1}$), the interacting system AM 1353–272, nicknamed the “The Dentist’s Chair” for its peculiar morphology, consists of three apparent components (see Fig. 1): A, a disturbed galaxy with two ~ 40 kpc long tidal tails (also cataloged as ESO 510-G 020G and IRAS F13533–2721), B, a disturbed edge-on disk galaxy, and C, an elliptical galaxy (see Weilbacher et al. 2000). While components A and B are a physical pair with a central velocity difference of only $\sim 150 \text{ km s}^{-1}$, C has a heliocentric velocity of $14,750 \text{ km s}^{-1}$ and is therefore located 38 Mpc behind the interacting pair. The tidal tails of AM 1353–272A host several blue knots with luminosities of dwarf galaxies. From their location and colors, they were identified by Weilbacher et al. (2000) as tidal dwarf galaxy (TDG) candidates.

In this Letter, we present the first evidence from deep optical spectroscopy with the Very Large Telescope (VLT) that some dense structures in the tidal tails are kinematically decoupled from the overall motion of the tails. Forthcoming instruments on large telescopes—e.g., high-resolution integral field spectrographs—will be very well suited to further investigate the specific dynamics in the tidal tails of AM 1353–272A.

2. OBSERVATIONS AND DATA REDUCTION

We have obtained multiobject spectroscopic data of a field centered on the system AM 1353–272 with the FOCAL REDUCER/LOW DISPERSION SPECTROGRAPH 2 (FORS2) instrument at the fourth VLT telescope, “Yepun.” Service mode observations were carried out in the night of 2001 August 13/14 under photometric conditions. Several spectroscopic standards were observed. The total exposure time of 3210 s was split into three individual exposures of 1070 s to ease cosmic-ray cleaning. The seeing of $1''$ is well sampled by an instrumental scale of $0''.2 \text{ pixel}^{-1}$. The grism 600B+22 was used, giving a wavelength coverage of 3450–5900 Å and a spectral resolution of 5.7 Å (1.2 Å pixel^{-1}) for a central slit of $1''$ width. We created a mask for the mask exchange unit of the FORS2 instrument with curved and tilted slits to cover the tails of AM 1353–272A and several surrounding galaxies in one setup (see Fig. 1).

The data reduction followed standard recipes, for which we used our own IRAF task MOSX (Weilbacher, Duc, & Fritze-v. Alvensleben 2002). Special care was taken to correct the curvature of the two-dimensional spectra of the curved slits: a proper wavelength calibration was carried out at each position along the slits, using a reference HeHgCd frame observed through the same mask as the science frames. The typical accuracy for each column is 0.04 Å rms . A fourth-order polynomial fit was then performed for each slit to determine the final wavelength solution and compute the parameters of the curvature correction. All these tasks were performed using the standard tools in the IRAF package LONGSLIT. The result of this procedure is presented in Figure 2: the original, uncorrected two-dimensional spectrum is compared with the spectrum after the correction.

After subtracting the sky background, we used the brightest emission lines from the slits along the tidal tails to derive the velocity profiles with an IRAF script based on the FITPROFS procedure. As a check, the same velocity fit was carried out with the nearest lines in the wavelength calibration spectrum. The 1σ differences from zero velocity in this control fit are below 1 km s^{-1} . The *relative systematic* errors in the final velocity profiles should be on the order of 1 km s^{-1} , while the errors for single points are typically 15 km s^{-1} .

3. RESULTS

Figure 3 presents the velocity distribution of the ionized gas along the two tails of AM 1353–272. The velocities indicated

¹ Based on observations collected at the European Southern Observatory, La Silla, Chile (ESO 67.B-0049).

² Universitäts-Sternwarte, Geismarlandstrasse 11, 37083 Göttingen, Germany; weilbach@uni-sw.gwdg.de, ufritze@uni-sw.gwdg.de.

³ Centre National de la Recherche Scientifique, URA 2052, and CEA, DSM, DAPNIA, Service d’Astrophysique, Centre d’Etudes de Saclay, 91191 Gif-sur-Yvette Cedex, France; paduc@cea.fr.

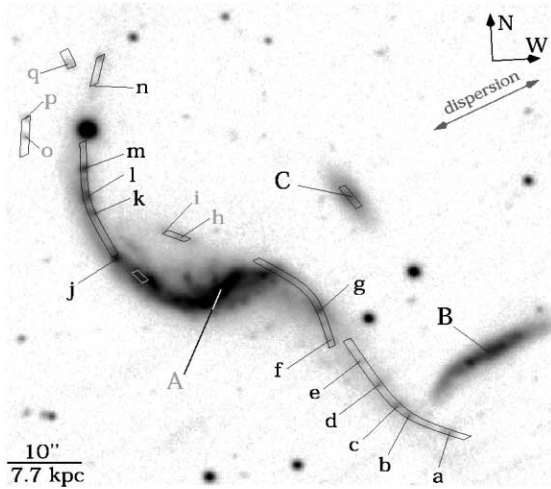


FIG. 1.—Finding chart of AM 1353–272. Original B -band image from the SUSI camera at the New Technology Telescope (Weilbacher et al. 2000) in logarithmic scale. The field of view is $\sim 2' \times 2'$. Black labels mark objects with measured redshift. [See the electronic edition of the Journal for a color version of this figure.]

on the top of Figure 3 are relative to the interpolated central velocity $V_A = 11,935 \text{ km s}^{-1}$ of AM 1353–272A. The relative $H\beta$ flux and hence distribution of the $H \text{ II}$ regions along the tails is shown below: it may be used to infer the signal-to-noise ratio (S/N) of the emission lines used to derive the velocities. Vertical lines mark the individual optical knots studied by Weilbacher et al. (2000). Note that nearly all of them are sites of active star formation, as predicted by a comparison of photometric starburst models with optical broadband colors.

At first glance, it seems as if there are velocity gradients within the knots and sudden jumps in velocity between them.

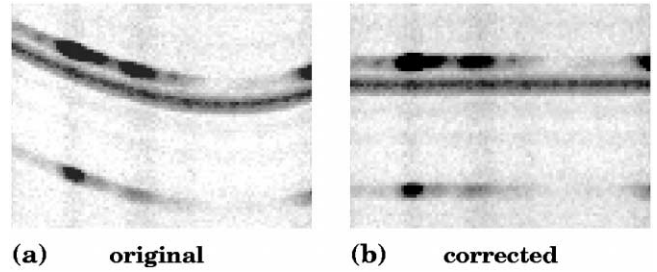


FIG. 2.—Slit curvature correction. As an example, we show part of a two-dimensional spectrum with the emission lines $[O \text{ III}] \lambda\lambda 5007, 4959$ emitted by knots j – m . Between these object lines, a skyline is visible that allows us to visually judge the quality of the correction. [See the electronic edition of the Journal for a color version of this figure.]

To further analyze the steplike shape of the velocity curve, we subtract the overall streaming motion of the tails, by fitting a fifth-order cubic spline (using IRAF's CURFIT task) to all velocity points. We then extract individual regions from the residual velocity field (see lower part of Fig. 3). In order to quantify the remaining apparent velocity gradients, we tried to fit a linear relation to all velocity gradients within the spatial extent of the knots. The results are given in Table 1, together with the error given by the fit procedure, the maximum velocity difference ΔV_{max} , and the angular extent of the fitted gradients. The fits seem to be a good first-order approximation to the real velocity gradients in most cases and are shown in the bottom part of Figure 3. Seven knots show velocity amplitudes that are significant, with errors below 50%. They reach 340 km s^{-1} for object a . For several knots, the gradient is also clearly resolved, i.e., it is observed to extend more than twice the seeing of $1''$.

4. DISCUSSION AND CONCLUSIONS

Given the observed significant velocity gradients within seven knots of the tails of AM 1353–272A, we discuss several possibilities of the origin of this specific velocity distribution.

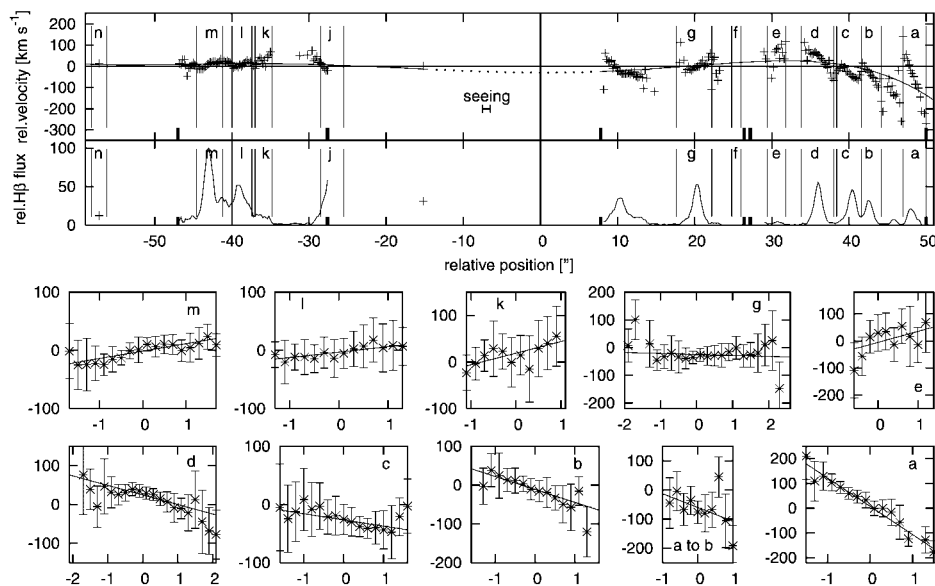


FIG. 3.—Velocities along AM 1353–272A. *Top*: Velocity field relative to a zero point of $11,935 \text{ km s}^{-1}$ along the ridge of the galaxy from the northern (*left*) to the southwestern (*right*) tip of the tidal tail. The seeing of $1''$ is indicated. The lower part shows the $H\beta$ flux in relative units on the same spatial scale. The size of each knot is marked with vertical lines. Thick lines on the position axis indicate the ends of the curved slits. A fifth-order fit to the overall velocity profile is shown. *Bottom*: Extracted residual velocity field of each knot after correction for tidal motion, plotted as relative position (in units of arcseconds) vs. relative velocity (in units of kilometers per second). Lines show a linear fit. [See the electronic edition of the Journal for a color version of this figure.]

TABLE 1
VELOCITY GRADIENTS WITHIN THE KNOTS

Identification ^a	ΔV_{\max}^b (km s ⁻¹)	Error (%)	Extent ^c (arcsec, kpc)
<i>a</i>	+343	5	3.0, 2.3
<i>a-to-b</i> ^d	+94	72	2.0, 1.5
<i>b</i>	+87	21	2.6, 2.0
<i>c</i>	+34	40	3.2, 2.5
<i>d</i>	+93	10	4.2, 2.9
<i>e</i>	-73	65	2.4, 1.4
<i>f</i> ^e
<i>g</i>	+15	170	4.6, 3.2
<i>k</i>	-50	31	2.2, 1.7
<i>l</i>	-24	24	2.6, 2.0
<i>m</i>	-43	19	3.4, 2.6

^a Knots with significant amplitude of velocity gradient are marked in boldface.

^b Gradients with positive sign have the highest velocity toward the north of the system.

^c The seeing of 1" at the distance of AM 1353-272A corresponds to ~800 pc.

^d We designate the region $\pm 1''$ around $+45''8$ distance from the nucleus as *a-to-b*.

^e Low S/N.

Instrumental errors can be excluded as a cause of these gradients. The velocity profiles observed over very small angular sizes (a few arcseconds) cannot be explained with flexures or distortions of the instrument. The wavelength calibration has been carried out and checked with the procedure described in § 2. As a result, any *relative* instrumental effects within a given slit should be below 1 km s⁻¹.

The apparent gradients could result from projection effects. As the angular size probed is only about 2–4 times the seeing, several smaller, physically unrelated knots might appear blended into one larger clump, mimicking the gradient we observe. It seems improbable, however, that this should be the case for many knots. Besides the two well-determined tidal tails, there is no indication of complex tidal structures in this system. It is therefore quite unlikely that tidal debris outside the well-defined tails is observed in projection close to so many tidal knots. Projection effects within a single tail are possible. First, the tails may have some depth along the line of sight, as can be seen in dynamical models of interactions, starting with the idea of Toomre & Toomre (1972) to view tails as two-dimensional ribbons. Second, the very tip of the southern tail could indeed be bent. Its three-dimensional shape might partly account for the exceptionally large velocity gradient observed toward condensation *a*. An example of a projection by such a bend near the end of a tail is discussed by Hibbard et al. (2001) for the tail of the Antennae galaxies (NGC 4038/39). There, the total H I column density and the velocity dispersion along the line of sight mimic a massive condensation of matter. In their high-resolution H I data, they find two gas concentrations at different velocities, which have only about a tenth of the originally estimated mass. The amplitude $\Delta V_{\max} = 340$ km s⁻¹ within knot *a* (compared to $\Delta V_{\max} \sim 50$ – 100 km s⁻¹ in the Antennae region) makes it seem unlikely to be caused by projection alone. The overall velocity field toward the end of the southern tail is decreasing. If the tail was bent backward to the center, one would expect this trend to continue. Knots projected from this bent part of the tail should then have even lower velocity than *a*. Such velocities are not observed. Projection

effects by a bent tail for other knots apart from *a* are implausible.

Velocity gradients could, in principle, be caused by gaseous outflows where one side of an expanding shell is blocked by dust. This would require significant amounts of extinction within the knots, while we find only very moderate absorption ($A_B \lesssim 1.0$ mag, including galactic $A_B = 0.26$ mag, estimated from Balmer line ratios). In addition, an outflow would also imply line-broadening. There is no indication of broad lines here, as the FWHM of the H β line is the same as the spectral resolution. It is very unlikely that the gradients are caused by outflows.

Rotation of bound objects could also create this kind of velocity gradient. From the irregular optical appearance and the location of the knots within tidal tails, it is unlikely that the stars in the potential of a knot have stable orbits. True Keplerian motion will not apply here, and it would then be premature to interpret the observed kinematics in terms of "rotation." Mass estimates from the Virial theorem would strongly overestimate the real mass contained within the knots.⁴

Instead, we may be witnessing the formation of bound objects in the tidal tails that are not yet virialized. The velocity gradients also seem to be specifically oriented in the sense that the higher velocity end of each knot points toward the center of AM 1353-272A. A possible cause could be the rotational direction of the progenitor disk before the interaction. The presence of the companion galaxy B near the southwestern tidal tail could also amplify motions in the tails, to create a "spin" in these knots in one direction. This would also explain the higher velocity amplitudes within the knots in the southwestern tail close to the companion.

The idea of TDGs—dwarf galaxies that are born as condensations in tidal tails—has been discussed in recent years by several authors (Barnes & Hernquist 1992; Hibbard & Mihos 1995; Duc et al. 1997), both theoretically and observationally. Duc et al. (2000) proposed a first definition of the term TDG as a self-gravitating object of dwarf galaxy mass formed from tidal material (see also Weilbacher & Duc 2001). While we are hampered by the spatial resolution and cannot give the ultimate proof of the velocity gradients as motion of tidal material beginning to get bound into knots, it seems that we are witnessing the formation of TDGs in the tails of AM 1353-272A, for the first time for multiple objects along both tails of the same interacting galaxy.

Forthcoming instruments for high-resolution spectroscopy on 8 m class telescopes, e.g., integral field instruments, will enable us to confirm the velocity gradients and further investigate their origin. Coupled with the high spatial resolution of adaptive optics, these instruments will be very useful tools to analyze the unique properties of the knots seen in these tidal tails. To fully understand the geometry and interaction parameters causing this first series of possibly genuine TDGs and to complement the observations, detailed dynamical *N*-body + smoothed particle hydrodynamics modeling of the collision will be necessary.

We thank I. Appenzeller for help with the proposal and data retrieval and our anonymous referee for a friendly and helpful report. P. M. W. is partly supported by DFG grant FR 916/6-2.

⁴ If caused by Keplerian rotation alone, the rotational velocity of knot *a* would be of the same order as those of giant spiral galaxies, which is unrealistic for an object with $M_B = -13.7$ mag.

REFERENCES

- Barnes, J., & Hernquist, L. 1992, *Nature*, 360, 715
Duc, P.-A., Brinks, E., Wink, J., & Mirabel, I. 1997, *A&A*, 326, 537
Duc, P.-A., et al. 2000, *AJ*, 120, 1238
Hibbard, J. E., & Mihos, J. 1995, *AJ*, 110, 140
Hibbard, J. E., van der Hulst, J. M., Barnes, J. E., & Rich, R. M. 2001, *AJ*, 122, 2969
Springel, V., & White, S. D. M. 1999, *MNRAS*, 307, 162
Toomre, A., & Toomre, J. 1972, *ApJ*, 178, 623
Weilbacher, P. M., & Duc, P.-A. 2001, in *Dwarf Galaxies and Their Environment*, ed. K. de Boer, R.-J. Dettmar, & U. Klein (Aachen: Shaker), 269
Weilbacher, P. M., Duc, P.-A., & Fritze-v. Alvensleben, U. 2002, *A&A*, submitted
Weilbacher, P. M., Duc, P.-A., Fritze-v. Alvensleben, U., Martin, P., & Fricke, K. J. 2000, *A&A*, 358, 819